

RESEARCH ARTICLE

10.1002/2017GC007219

Key Points:

- The presence of exsolved volatiles changes the thermal evolution of a magma reservoir
- Exsolved volatiles allow for a stronger temperature increase during recharge events leading up to eruption
- The eruptive style at Volcán Quizapu is explained through changes in exsolved volatile content in the magma chamber

Correspondence to:

W. Degruyter,
degruyterw@cardiff.ac.uk

Citation:

Degruyter, W., Huber, C., Bachmann, O., Cooper, K. M., & Kent, A. J. R. (2017). Influence of exsolved volatiles on reheating silicic magmas by recharge and consequences for eruptive style at Volcán Quizapu (Chile). *Geochemistry, Geophysics, Geosystems*, 18, 4123–4135. <https://doi.org/10.1002/2017GC007219>

Received 5 SEP 2017

Accepted 23 OCT 2017

Accepted article online 1 NOV 2017

Published online 24 NOV 2017

Influence of Exsolved Volatiles on Reheating Silicic Magmas by Recharge and Consequences for Eruptive Style at Volcán Quizapu (Chile)

W. Degruyter¹ , C. Huber², O. Bachmann³ , K. M. Cooper⁴ , and A. J. R. Kent⁵

¹School of Earth and Ocean Sciences, Cardiff University, Cardiff, Wales, UK, ²Department of Earth, Environmental and Planetary Sciences, Brown University, Providence, RI, USA, ³Institute of Geochemistry and Petrology, ETH Zurich, Zurich, Switzerland, ⁴Department of Earth and Planetary Sciences, University of California, Davis, Davis, CA, USA, ⁵College of Earth, Ocean, and Atmospheric Sciences, Oregon State University, Corvallis, OR, USA

Abstract The two most recent eruptions of Volcán Quizapu (southern Andes, Chile), only 85 years apart, were both triggered by magma recharge and extruded the same volume (about 5 km³) of the same volatile-rich dacitic magma, but showed a remarkable shift from effusive (1846–1847) to explosive (1932) behavior. We demonstrate, using a newly developed model, that the presence or absence of an exsolved volatile phase in the reservoir strongly influences its mechanical and thermal response to new inputs of magma. We propose that, prior to the 1846–1847 effusive eruption, gas bubbles damped the build-up of excess pressure and allowed recharge of a significant volume of magma before triggering the 1846–1847 eruption. The strong temperature increase that resulted enhanced syneruptive outgassing leading to an effusive eruption. In contrast, during the repose period between the 1847 and 1932 eruptions, new recharges found a much less compressible host reservoir as the exsolved gas phase was largely removed in response to the prior eruption, yielding rapid pressurization, minor reheating, and comparatively less syneruptive outgassing. The combination of these effects culminated in an explosive eruption.

1. Introduction

Magma recharge into a shallow magma reservoir has often been inferred as a source for surface deformation at active volcanic centers and a potential trigger for eruptions (Blake, 1981; Johnson, 1992; Pallister et al., 1992; Sparks et al., 1977; Watts et al., 1999). Recharges can lead to pressurization, inducing surface uplift and if a critical overpressure is exceeded, an eruption can follow. Simultaneously, recharge of new magma brings additional heat to the magma reservoir, leading to a temperature increase and partial melting of the crystalline material, as regularly observed in the petrological record (Bachmann & Dungan, 2002; Girard & Stix, 2009; Klemetti & Clyne, 2014; Koleszar et al., 2012; Molloy et al., 2008; Murphy et al., 2000; Till et al., 2015; Wiebe et al., 2004). However, the amount of reheating by recharge of a magma reservoir and its potential to pressurize and erupt are poorly quantified as these quantities are often considered independently. This connection between pressure and temperature changes has important implications for eruption frequency and erupted volume (Degruyter et al., 2016). Here, we will study how this link between the thermal and mechanical evolution of a magma reservoir influences the style of eruptions using the observations at Volcán Quizapu.

1.1. The Twin Eruptions at Volcán Quizapu

Quizapu is located in the Southern volcanic zone of the Andes, and is situated between Cerro Azul to its south and Descabezado Grande to its north (Figure 1). Its historical eruptions (1846–1847 and 1932) are particularly well studied (Hildreth & Drake, 1992; Ruprecht & Bachmann, 2010; Ruprecht & Cooper, 2012; Ruprecht et al., 2012). We summarize the findings relevant for our purpose. Two significant outpourings of dacitic magma occurred within a relatively close time interval of about 85 years. The first eruption, in 1846–1847, was effusive, while the second, in 1932, led to an explosive Plinian event (Hildreth & Drake, 1992). Despite these different eruptive styles, the two deposits have similar volumes (~5 km³; Hildreth & Drake, 1992), bulk-rock composition (dacite; Hildreth & Drake, 1992), storage depth (130–180 MPa from magnesiohornblende; Ruprecht et al., 2012) and water content (4–6 wt % using plagioclase and amphibole

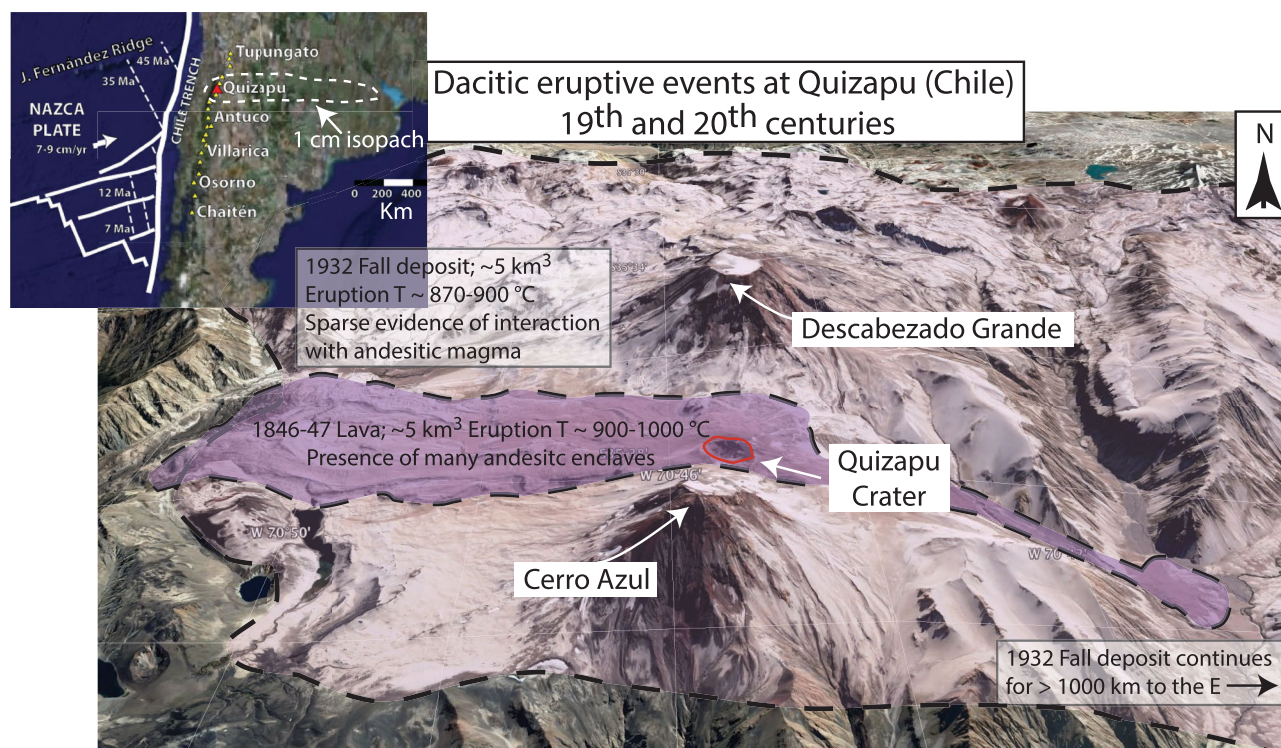


Figure 1. (top left inset) Google Earth image of the Quizapu location and regional area, showing both the 1846–1847 lava flow and the 1932 fall deposits. It allows a comparison of the variable extent of both deposits, despite their similar volume, and stresses the much higher content in mafic comagmatic enclaves in the lava. A 1 cm isopach from Hildreth and Drake (1992).

hygrometry; Ruprecht & Bachmann, 2010; Ruprecht et al., 2012). They also both show evidence of andesite recharge before the eruption (Hildreth & Drake, 1992; Ruprecht & Bachmann, 2010; Ruprecht et al., 2012). Despite these similarities, there are notable differences in (1) recharge volume and (2) preeruptive reheating (Ruprecht & Bachmann, 2010). The 1846–1847 lava flow shows abundant mafic enclaves (up to 20–30% volume in places) and a significant temperature increase (>50°C; using amphibole and Fe-Ti oxide geothermometry to estimate storage and preeruptive temperature, respectively) related to the recharge event, while the 1932 Plinian deposits show a limited amount of mafic recharge (only a thin layer of andesitic tephra present in the deposits) and a concomitant smaller increase in temperature (<10–20°C).

Volatiles play a major role in driving explosive volcanic eruptions, as they exsolve and rapidly expand upon decompression during ascent in the conduit. This creates a positive feedback between exsolution and decompression rate, accelerating the magma upward and ultimately ending in magma fragmentation. However, the development of permeable foam and/or fractures can create pathways for efficient gas escape, which can prevent acceleration and lead to an effusive eruption, even for gas-rich, viscous magmas (e.g., Castro et al., 2012; Degruyter et al., 2012; Eichelberger et al., 1986; Gonnermann & Manga, 2003; Jaupart & Allegre, 1991; Kozono & Koyaguchi, 2009; Villemant & Boudon, 1998; Woods & Koyaguchi, 1994). The temperature increase observed at Quizapu related to efficient mingling of the stored dacite with a 1100°C andesite recharge is thought to have lowered the viscosity of the magma enough to permit efficient gas escape during the 1846–1847 event, but not during the 1932 explosive event (Ruprecht & Bachmann, 2010). The critical question remains as to why a much smaller recharge event could have produced the necessary overpressure to lead to the 1932 eruption if all other conditions were similar. We hypothesize that the absence or presence of exsolved volatiles in the magma reservoir at the time of the recharge can strongly influence the response of magma to mafic recharge and lies at the heart of the change in behavior at Quizapu.

The role of volatiles (either dissolved in the melt, or exsolved as a gas phase) in the upper crustal magma storage region can strongly affect both pre and syneruptive processes (Cassidy et al., 2016; Degruyter et al.,

2016; Edmonds et al., 2014; Huppert & Woods, 2002; Parmigiani et al., 2016; Roggensack et al., 1997). In this study, we consider how the presence of an exsolved gas phase influences the response of a shallow magma body to magma recharge by employing a thermomechanical magma reservoir model. We demonstrate the marked influence of a preeruptive exsolved volatile phase on the temperature and pressure evolution in a shallow reservoir subjected to a recharge event and its potential impact on forthcoming eruptions. When applied to the “twin” eruptions of Quizapu, our model is able to explain the difference in thermal perturbation and eruptive style as an expression of the exsolved volatile content in the reservoir.

2. Magma Reservoir Modeling

We use the thermomechanical model described in Degruyter and Huber (2014) to determine the effect of exsolved volatiles on the short-term evolution of an upper crustal magma reservoir exposed to transient recharge events. We assume that the upper crustal magma reservoir is initially made up of a mobile portion (magma chamber) surrounded by a crystal mush that transitions into cold wall rocks and formed over tens to hundreds of thousands of years by incremental emplacement of magma (Annen, 2009; Gelman et al., 2013; Karakas et al., 2017). The properties of the magma are averaged over the size of the chamber and the melt, crystal, and gas phase are assumed to be in equilibrium. The governing equations of the model are the conservation of mass, conservation of water, and conservation of enthalpy combined with a set of closure equations, which include relationships for melting, solubility, and gas density. We consider an upper crustal magma reservoir that is representative of Quizapu conditions (Ruprecht & Bachmann, 2010; Ruprecht & Cooper, 2012; Ruprecht et al., 2012), and use a melting curve specific for dacitic composition following the parameterization of Huber et al. (2009), with a solidus at 700°C and a liquidus at 1020°C. The properties of the gas phase are calculated from a parameterized solubility law for water in rhyolite (see equation (B5), Appendix B; Dufek & Bergantz, 2005; Zhang, 1999) and a parameterized equation of state based on a modified Redlich-Kwong relationship (see equation (B6), Appendix B; Halbach & Chatterjee, 1982; Huber et al., 2010). This set of equations allow tracking the evolution of pressure, temperature, and volume of the chamber as well as the volume fractions and densities of the different phases (see Appendix A). We model the sharp changes in the thermomechanical state of the magma reservoir due to rapid (monthly to decadal) mass gain by recharge and mass removal during eruptions (Cooper & Kent, 2014; Degruyter et al., 2016; Druitt et al., 2012).

2.1. Initial Conditions

We consider two scenarios, one where the chamber initially contains a two-phase (melt + crystals) magma occupying a volume of 50 km³, the second is set up with a three-phase magma (with initial gas volume fraction between 0.05 and 0.15) that contains the same mass initially. There are no good constraints on the size of the magma chamber of Quizapu. However, based on the fact that a three-phase magma will approximately remove 5–10 wt. % of the magma chamber to return to lithostatic pressure (Bower & Woods, 1997; Degruyter et al., 2016), the initial volume of 50 km³ will produce eruptions that are on the same order as the observed erupted volumes of 5 km³ at Quizapu (Hildreth & Drake, 1992). The initial volume of the magma chamber is set to 50 km³ for all calculations, except those in Figure 6 where in one case it is set to 45 km³ to test the effect of volume change after the first eruption.

The initial pressure is set to 155 MPa, based on the pressure estimates from magnesiohornblende between 130 and 180 MPa (Ruprecht et al., 2012), which corresponds to a depth of about 6 km. We use an initial chamber temperature of 870°C based on the storage temperature estimated using amphibole geothermometry of 870 ± 30°C (Ruprecht & Bachmann, 2010). We assume an initial dissolved water content of 5 wt. % based on estimates from plagioclase and amphibole hygrometry between 4 and 6 wt. % (Ruprecht & Bachmann, 2010). Gas volume can build up through high initial water content, second boiling (Blake, 1984), but also through bubble migration from the highly crystalline surroundings to the crystal-poor magma chamber (Parmigiani et al., 2016). In the three-phase (melt + crystals + gas) magma, we start with an initial gas volume fraction of 0.1 and in the two-phase (melt + crystals) magma it is by definition zero. The melt and crystal phases have constant bulk moduli of 10 GPa and thermal expansion coefficients of 10⁻⁵/K such that these phases are nearly incompressible and their densities, with initial values $\rho_m = 2,400$ kg/m³ for melt and, $\rho_x = 2,750$ kg/m³ for crystals, are nearly constant throughout the calculations. The bulk modulus and thermal expansion of the gas phase are calculated explicitly from the equation of state of the gas phase (equation (B6) in Appendix B).

2.2. Boundary Conditions

The magma chamber loses heat to its surroundings. The rate of heat loss is calculated from an analytical solution of a sphere that sits in a larger spherical shell. The temperature of the inner sphere varies over time and is equal to that of the magma chamber. The outer boundary of the spherical shell is 10 times the radius of the initial chamber radius and has a temperature of 500°K or 227°C, which is the far-field temperature at the depth of the reservoir and corresponds to a geothermal gradient within the range of 30–35°C/km. This temperature profile is further used to calculate the effective viscosity of the surrounding shell, which is applied to describe the viscoelastic response of the crust to changes in stress in the reservoir following the description of Dragoni and Magnanensi (1989) and Jellinek and DePaolo (2003). This relationship governs the evolution of volume of the chamber (see equation (A4) in Appendix A).

The magma chamber can gain mass by recharge of new magma and lose mass through an eruption. The recharge magma has a temperature 1,100°C as inferred from Ruprecht and Bachmann (2010) and is assumed to be undersaturated in volatiles as it reaches the upper crustal reservoir. The duration and rate of emplacement are variable and range between 1 and 100 years and 0.2 and 0.01 km³/yr, respectively, in agreement with timescales and rates inferred from petrology and geophysics (Cooper & Kent, 2014; Druitt et al., 2012; Martin et al., 2008; Menand et al., 2015; Morgan et al., 2006; Parks et al., 2012). The magma that is removed from the chamber has the same physical properties as that within the chamber.

In order to produce an eruption, two conditions are required: (1) the magma needs to be mobile (i.e., it needs to be able to flow) and (2) the magma chamber needs to reach a critical overpressure to generate a pathway to the surface. The rheology of magma is complex and its ability to flow depends on a number of variables (i.e., composition, temperature, water content dissolved in the melt, crystal and gas volume fraction, and the stress state; see Mader et al., 2013 for a review). However, to a first order, a magma having less than ~50 vol. % crystals is typically considered mobile (Lejeune & Richet, 1995; Marsh, 1981). For the conditions considered in this study, the magma remains mobile throughout the calculations.

Common critical overpressure values used to start dyke propagation have a wide range between 1 and 100 MPa (Grosfils, 2007; Grosfils et al., 2015; Gudmundsson, 2012; Jellinek & DePaolo, 2003; Karlstrom et al., 2010; Rubin, 1995). If the overpressure is not large enough, dykes can get trapped in the crust before reaching the surface due to solidification, lack of volume, or low-density crustal layers (Rubin, 1995; Taisne et al., 2011). In order to ensure the dyke reaching the surface and initiating an eruption, a value of 40 MPa appears reasonable (Jellinek & DePaolo, 2003; Rubin, 1995) and is used here. A number of mechanisms can pressurize a chamber such as recharge of magma from deeper storage regions (Blake, 1981), second boiling (Blake, 1984; Stock et al., 2016; Tait et al., 1989), and buoyancy (Caricchi et al., 2014; Jellinek & DePaolo, 2003; Malfait et al., 2014). For very large systems, instabilities in the crustal roof rock induced by chamber pressurization might initiate an eruption (Gregg et al., 2012; Gudmundsson, 2012). Other proposed eruption trigger mechanisms include large earthquakes (Manga & Brodsky, 2006) and tectonic stresses (Allan et al., 2012). We focus our study on pressurization of the magma reservoir by recharge events, which is suggested to be the cause for the eruptions at Quizapu (Ruprecht & Bachmann, 2010). The rate of mass withdrawal during an eruption is set to a constant value of 10⁵ kg/s such that the characteristic timescale of eruption is much faster than the other processes considered. An eruption ceases when the pressure of the magma chamber returns to the lithostatic pressure.

3. Effect of Exsolved Volatiles on Reheating

We first explore recharge scenarios for which no eruption ensues to compare the magma reservoir response between a system that contains an exsolved volatile phase (three-phase) for a range of initial gas volume fraction between 0.05 and 0.15 and one that has no gas (two-phase). The change of thermal contribution to the enthalpy ΔH caused by the recharge can be written as

$$\Delta H = \Delta(\rho c T V) - L_m \Delta(\rho_X \varepsilon_X V) - L_e \Delta(m_{eq} \rho_m \varepsilon_m V), \quad (1)$$

with ρ , ρ_X , ρ_m being the density of the bulk, the crystals, and the melt; ε_X , ε_m the volume fraction of the crystal and melt phase; $L_m = 290$ kJ/kg, $L_e = 610$ kJ/kg the latent heat of melting and exsolution, using the values of Caricchi and Blundy (2015); c the bulk heat capacity, m_{eq} the dissolved water content in the melt phase, T the temperature, V the volume of the magma chamber, and Δ representing variations between

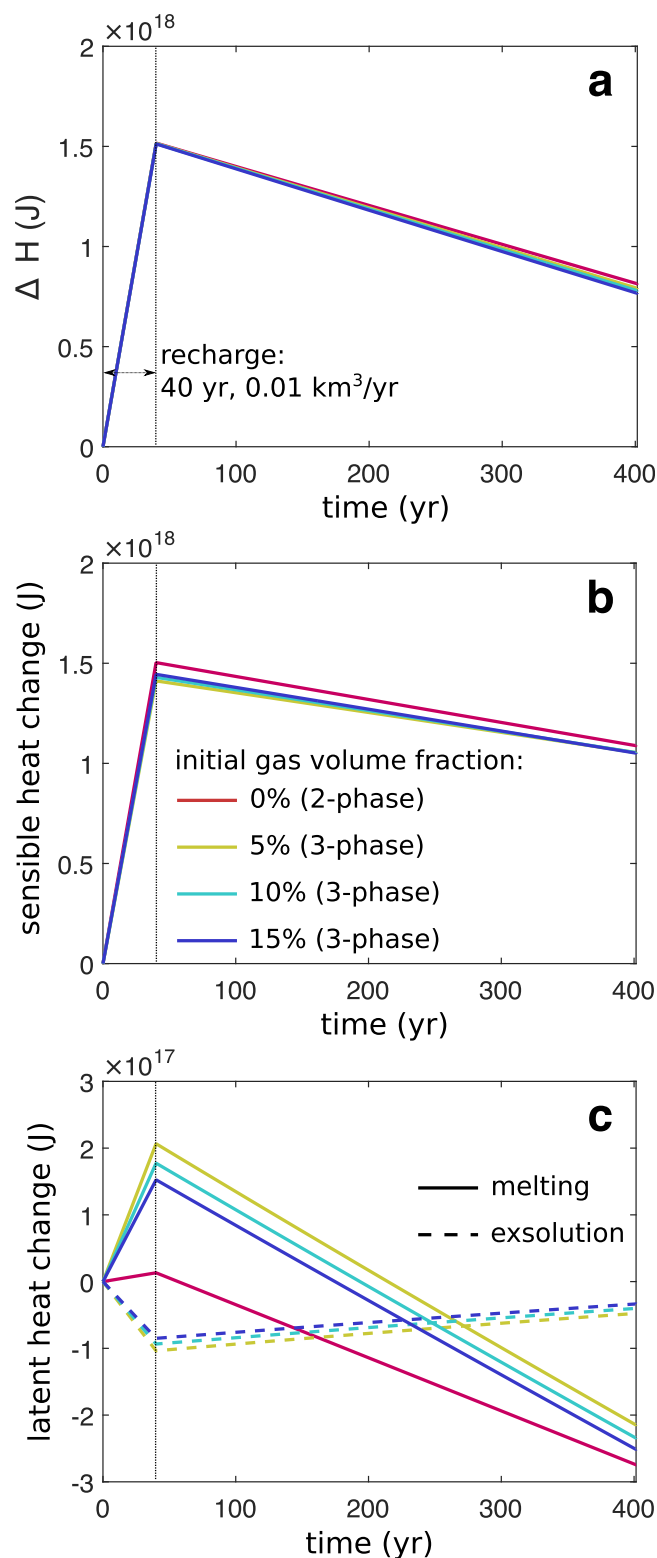


Figure 2. Changes in a magma reservoir's heat budget for a range of initial gas volume fractions in response to an identical recharge event. (a) Enthalpy (equation (1)), (b) sensible heat, and (c) latent heat change due to a recharge event with a duration of 40 years and an emplacement rate of $0.01 \text{ km}^3/\text{yr}$. The vertical dashed lines indicate the end of the recharge event.

two states. On the right-hand side of equation (1), the first term is the sensible heat change in the system, the second term represents the latent heat contribution associated with crystallization or melting and the last is the latent heat change caused by the exsolution or dissolution of water. In the case where the recharge does not lead to an eruption, as in the representative example shown in Figure 2, the thermal budget is influenced by (i) a heat source provided by the recharge event and (ii) a heat sink due to heat conduction driven by the temperature difference with the colder surrounding crust.

Although the heat budget changes little between a two-phase and three-phase magma ($\Delta H_{2p} \approx \Delta H_{3p}$, Figure 2a), the latent and sensible heats are partitioned differently (Figures 2b and 2c) and lead to a different temperature response of the system (Figure 3b). In the two-phase system, the heat budget is simply partitioned between the sensible heat of the magma mixture and the latent heat of melting. During a recharge event, there is a net gain in the enthalpy budget, which leads to melting and consumes part of the enthalpy injected by the new magma. The rest (and majority) of the enthalpy is converted to an increase of sensible heat. This is controlled by the phase diagram (melting curve) and latent heat values used (see Appendix A). In a three-phase system, the compression of the magma during recharge leads to partial resorption of water in the melt, which releases latent heat. This energy, together with the enthalpy from the recharge, is then allocated to melting and an increase in sensible heat. Compared to the two-phase system, the sensible heat is very similar, but the amount of melting is significantly higher. When the recharge event ceases, the opposite effect takes place (i.e., crystallization is more rapid in the three-phase magma during cooling).

The change in overall sensible heat depends on the change in mass, the mixture heat capacity c , and the temperature T . Using the same mass of recharge, we can focus on the evolution of the latter two properties (c and T) for both systems (Figures 3b and 3d). Exsolved water has a heat capacity $c_g = 3,900 \text{ J/kg/K}$ that is about 3.5 times greater than either crystal ($c_x = 1,315 \text{ J/kg/K}$) or melt phases ($c_m = 1,205 \text{ J/kg/K}$) using values obtained by Caricchi and Blundy (2015). Hence, the capacity to store heat of the magma mixture c is significantly different between a two-phase and a three-phase magma as it is described by the weighted average of the heat capacity of the different phases:

$$c = \frac{\rho_x \epsilon_x c_x + \rho_g \epsilon_g c_g + \rho_m \epsilon_m c_m}{\rho}, \quad (2)$$

using the same symbols as above, with subscript g referring to the gas phase. The sensible heat does not change much between a two-phase and three-phase system (Figure 2b), but as the mixture heat capacity decreases more sharply in the three-phase system, a more pronounced temperature increase is observed in the three-phase system (about 3 times higher for the representative example in Figure 3). Although the amount of temperature difference does not appear to be large on the timescale of a single recharge event, these differences can accumulate over longer timescales and lead to very different magma reservoir histories as a result. Also note that the initial amount of gas has little influence compared to having no gas (Figures 2 and 3). Additionally, the pressure evolution (Figure 3a) is strongly different between a

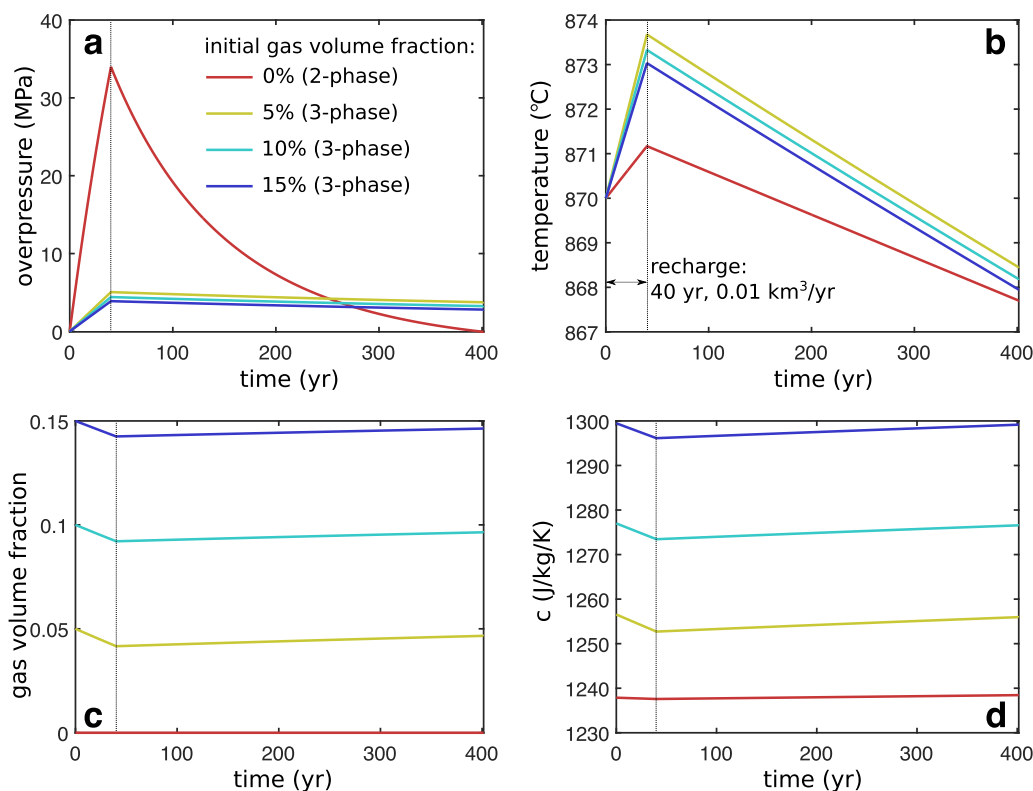


Figure 3. Response of a reservoir with a range of initial gas volume fraction to an identical recharge event. (a) Pressure, (b) temperature, (c) gas volume fraction, and (d) mixture heat capacity (equation (2)) change in response to a recharge with a duration and 40 years and magma emplacement rate of $0.01 \text{ km}^3/\text{yr}$ as in Figure 2. The vertical lines indicates the end of the recharge event.

two-phase system relative to the three-phase system, while there is little difference in pressure response within the three-phase calculations across a range of initial gas volume fractions (Figure 3c).

A comparison between recharge scenarios of similar rate and duration is not well suited for the situation at Quizapu as we need to compare recharge events that trigger an eruption. The change in magma compressibility and thermal expansion between two and three-phase systems leads to eruptions with different durations and mass fluxes following recharge events (Degruyter et al., 2016; Huppert & Woods, 2002; Rivalta & Segall, 2008). The recharge volume that needs to be emplaced to reach a given critical overpressure is much larger for a three-phase than a two-phase system (Degruyter et al., 2016). Thus, we need to implement recharge scenarios that produce a similar pressure signal over a similar timespan (by adjusting the rate of the recharge event; Figure 4). Due to the much larger amount of recharge needed in the case of the three-phase system (in this scenario about 7 times), the temperature increase is more pronounced compared to the temperature increase of the two-phase system (in this scenario more than 20 times). The higher compressibility and thermal expansion of bubble-bearing magmas permit more heat to be delivered preceding an eruption and amplifies the role of volatiles on the heat balance that was discussed for the example that did not lead to eruption. Alternatively, recharge scenarios with different duration, but having the same rates can also produce an eruption, which result in a very similar temperature change prior to eruption, but produce a very different pressure response (see Figure 5). The eruption itself lowers the temperature sharply due to the removal of mass and the heat it carries.

In the case of a three-phase magma, the decompression associated with an eruption allows for more exsolution of volatiles lowering the temperature to a greater amount than the two-phase magma. In both cases, an eruption returns the chamber temperature to a value closer to the storage temperature prior to the recharge event (Figure 5a). Finally, we also tested the effect of initial chamber volume to examine if the mass removal of 5 km^3 of the first eruption at Quizapu, had any influence on the capability of the magma

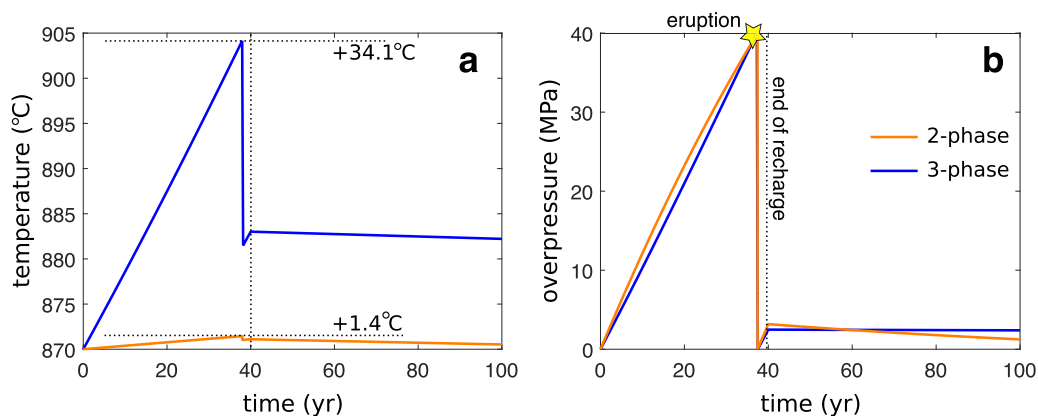


Figure 4. Response of a reservoir subjected to a recharge event with similar pressure evolution. (a) Temperature and (b) overpressure evolution of a magma reservoir that is exposed to a recharge event leading to eruption. The duration of both calculations is identical (40 years), while the rate is adjusted such that the pressure profiles closely match. The recharge rate for the two-phase magma is 0.0125 km³/yr and it is 0.09 km³/yr for the three-phase magma. The initial gas volume fraction for the three-phase magma is 0.1.

chamber to pressurize and reheat prior to the second eruption at Quizapu (Figure 6). We find this has only a minor influence on the pressure and temperature evolution leading up to the eruption.

4. Reservoir Evolution at Quizapu

From our results, we propose the following conceptual model for the magma reservoir evolution at Quizapu (Figure 7):

1. The Quizapu magma reservoir grew for a significant time (>10³ years; Ruprecht & Cooper, 2012) and reached a mobile volume of approximately several tens of cubic kilometers in size. In this period, gas bubbles started to form in the magma reservoir through second boiling and they accumulated in the mobile portion, i.e., the magma chamber (Parmigiani et al., 2016).
2. The magma chamber containing gas bubbles was exposed to a recharge event before the 1846–1847 eruptions. Based on timescales obtained from element diffusion in minerals at multiple volcanic systems, such recharge events likely lasted months to decades (Druitt et al., 2012; Martin et al., 2008; Morgan et al., 2006). The recharge event reheated the system significantly (by >50°C) and led to a mass gain > 10%, according to petrological observations (Ruprecht & Bachmann, 2010) and corroborated by the

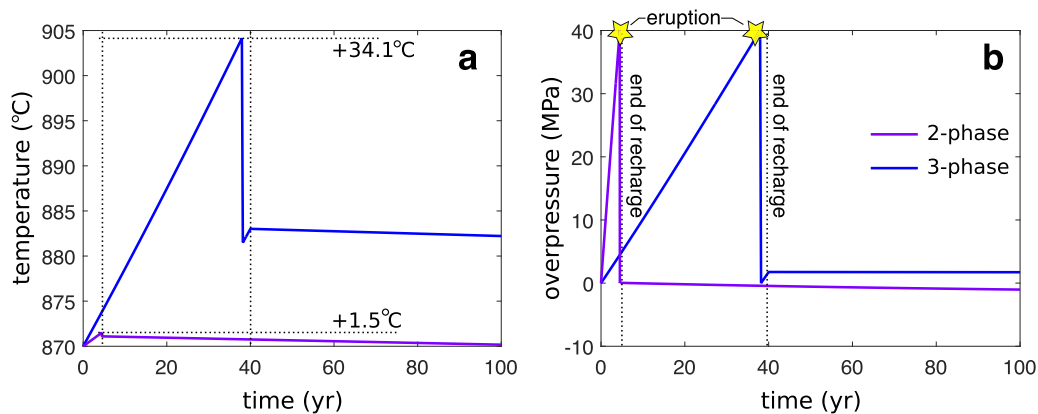


Figure 5. Response of a reservoir subjected to a recharge event with similar injection rate. Comparison between response of two- and three-phase (with initial gas volume fraction 0.1) magmas to recharge scenarios with the same recharge rate, and different duration leading up to an eruption. The recharge rate in both scenarios is 0.09 km³/yr. In the case of the three-phase magma, the recharge duration is 40 years (same as in Figure 4). In the case of the two-phase magma, a recharge event of only 4.5 years is necessary to produce an eruption. Although the rate is the same, the pressure response and thus the resulting surface deformation will be strongly different.

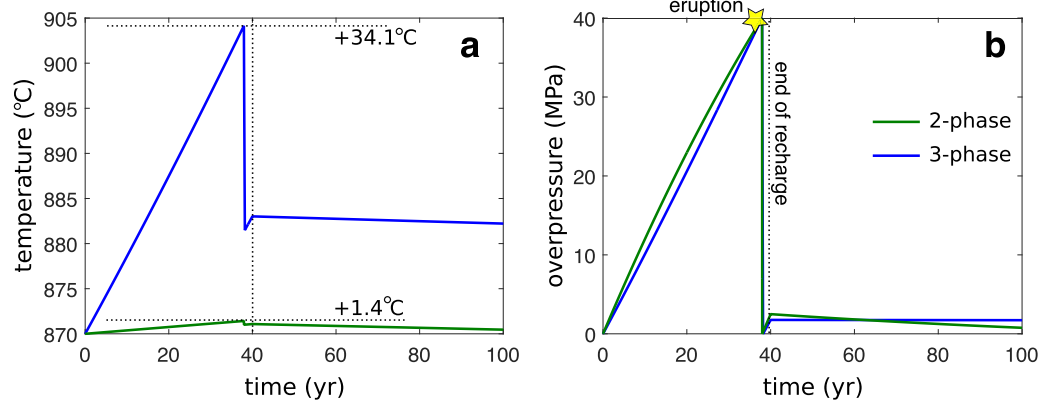


Figure 6. Effect of initial chamber volume on response of a magma reservoir. Comparison between response of two and three-phase (with initial gas volume fraction 0.1) magmas to recharge scenarios with the same recharge duration, and different emplacement rate leading up to an eruption. The initial volume of the two-phase magma is reduced to 45 km³ to test the effect of the 5 km³ volume loss related to the 1846–1847 eruption at Quizapu on the thermomechanical evolution of the magma reservoir. The duration of the recharge is 40 years. For the three-phase magma, the recharge rate is 0.09 km³/yr (same as in Figures 4 and 5). The two-phase magma is exposed to a recharge rate of 0.011 km³/yr in order to produce the same pressure signal as the three-phase magma. This is slightly lower than the 0.125 km³/yr necessary for the same initial volume in Figure 2. Hence, the effect of volume reduction has only a second-order effect. In addition, the effect on the temperature change (see Figure 4) is minor.

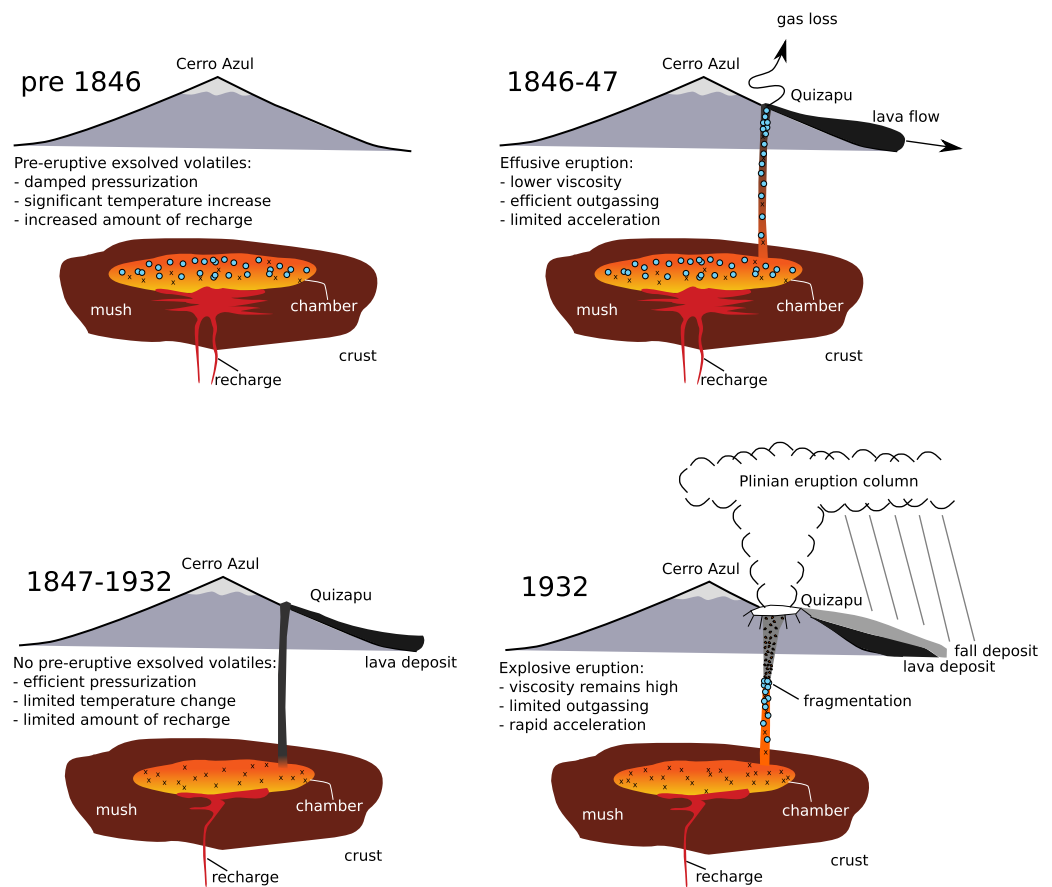


Figure 7. Conceptual model for the evolution of the Quizapu plumbing system producing the twin eruptions (not to scale). See section 4 for detailed explanation.

results of our model (i.e., the temperature change in magma with gas bubbles can be more than an order of magnitude stronger than magma without). Model calculations and scaling suggest a minimum gas volume fraction of about 0.07 prior to recharge is required for this behavior (see Appendix B). Below this amount of gas bubbles, the recharge event would pressurize the system up to a point where all the bubbles dissolve back into the melt prior to reaching the critical overpressure. The temperature changes found using petrological techniques are larger than the model calculations, which can be attributed to the spatial variations that exist at the hand-sample scale (in particular the addition of latent heat released by the crystallization of the andesitic enclaves, Ruprecht & Bachmann, 2010), while the model calculates a volume-averaged temperature at the reservoir scale.

3. The recharge event lasted sufficiently long and its rate was large enough to build a critical overpressure to nucleate and propagate a dike that reached the surface, and produced the 1846–1847 lava flow, as the temperature increase lowered the melt viscosity, and allowed a more efficient outgassing during ascent (Ruprecht & Bachmann, 2010). The minimum mass emplacement rate \dot{M}_{in} for such a recharge event can be estimated using scaling. In order for the crust to respond elastically, we require that the timescale of injection (τ_{in}) is faster than the viscous relaxation timescale (τ_{relax}):

$$\frac{\tau_{relax}}{\tau_{in}} = \frac{\dot{M}_{in}\eta_r}{M_0(\Delta P)_c} > 1, \quad (3)$$

with M_0 the initial mass of the chamber on the order of 10^{14} kg, $(\Delta P)_c$ the critical overpressure of 40 MPa, and η_r the viscosity of the chamber surroundings on the order of 2×10^{19} Pa s. Using these values, we get an estimate of 200 kg/s for \dot{M}_{in} . Assuming, the density of the injected magma is 2,400 kg/m³, we get a minimum volume emplacement rate of $\sim 3 \times 10^{-3}$ km³/yr that is required for pressurization. Similarly, we can estimate the volume change ΔV necessary to produce sufficient overpressure. Based on equation (A4) in Appendix A, we can estimate the volume as

$$\Delta V = \frac{(\Delta P)_c V_0}{\beta_{eff}} > 1, \quad (4)$$

with V_0 the initial volume of the chamber of 50 km³ and β_{eff} the effective bulk modulus of the magma, which in our calculations is on the order of 7×10^8 Pa for a three phase magma (Huppert & Woods, 2002). We thus require a volume of at least ~ 3 km³ to be emplaced for an eruption to occur. If the volume emplacement rate \dot{V}_{in} is known, we can estimate the duration τ_d until sufficient pressure is accumulated in the magma chamber as follows $\tau_d \sim \dot{V}_{in}/3$ km³.

4. The eruption significantly cooled the magma reservoir, which almost returned to its prerecharge temperature (as shown by the calculations in Figures 4–6). We propose that syn and posteruptive degassing during this first phase of activity removed most or even all exsolved volatiles from the magmatic system, while the melt remained at or near volatile saturation.
5. An additional recharge event produced a limited mass gain of less than one percent and temperature change of a couple of degrees prior to eruption as efficient pressurization was facilitated by the paucity or lack of exsolved volatiles in the system. Similarly, as above, this behavior would occur for a magma containing less than about 0.07 gas bubbles prior to the recharge event.
6. This recharge event led to an explosive eruption as magma viscosity was almost an order of magnitude greater than in 1846 due to a lower temperature (Ruprecht & Bachmann, 2010). This hindered permeability development and syneruptive outgassing. Fast syneruptive decompression during the explosive phase led to rapid exsolution in the chamber, which in turn induced excavation of a volume comparable to the previous effusive eruption (Huppert & Woods, 2002).

5. Conclusions

The presence of exsolved volatiles in subvolcanic magma reservoirs has three important effects on the thermomechanical response to magma recharges: (i) the dissolution of exsolved volatiles releases heat that can be used for melting preexisting crystals and increasing the sensible heat; (ii) water (dominant in the volatile phase) has a high heat capacity, and the dissolution of volatiles leads to a decrease in mixture heat capacity and therefore greater temperature changes; and (iii) a magma reservoir that contains bubbles requires more recharge mass to reach the critical overpressure, allowing more heat to be delivered prior to eruption

as well as magnifying the effects of (i) and (ii). Our results demonstrate that preeruptive conditions in the magma reservoir have important implications on the eruptive style. In particular, they lead to the counterintuitive implication that the presence of more volatiles in a shallow magma storage does not necessarily imply a more explosive behavior. Additionally, preexsolved volatiles can affect the rheology of magma and change its mobility (Pistone et al., 2012; Truby et al., 2015; Vona et al., 2017). Unraveling the preeruptive conditions of a magma reservoir of past eruptions will thus benefit greatly from a petrological assessment of the volatile saturation (e.g., Stock et al., 2016). Moreover, we note that observing surface deformation during volcano unrest (a proxy for pressurization in the magma reservoir) cannot be linked to a unique amount of recharge getting into the system and, even less to a prediction of presumed future eruption style. This is because depending on the abundance of exsolved volatiles, the dynamical evolution of a reservoir upon recharges and the related surface deformation signals can strongly vary. A more informed hazard assessment must incorporate a better characterization of the reservoir's conditions, including the amount of exsolved volatiles (e.g., Kilbride et al., 2016).

Appendix A: Magma Reservoir Model Description

The details of the model have been published and applied in Degruyter and Huber (2014); Degruyter et al. (2016); Parmigiani et al. (2017). Here we summarize the governing equations and the most relevant closure equations. The magma reservoir model is a lumped parameter model that solves for the conservation of mass, water, and enthalpy, which we can write in a condensed form as:

$$\frac{dM}{dt} = \dot{M}_{in} - \dot{M}_{out}, \quad (A1)$$

$$\frac{dM^w}{dt} = \dot{M}_{in}^w - \dot{M}_{out}^w, \quad (A2)$$

$$\frac{dH}{dt} = \dot{H}_{in} - \dot{H}_{out}, \quad (A3)$$

with M , M^w , and H the (total) mass, the water mass and the enthalpy of the magma chamber, respectively. The index "in" refers to source terms, while "out" indicates sink terms. We add three additional ordinary differential equations to describe the evolution of the magma chamber volume (V), melt (ρ_m), and crystal density (ρ_X) as follows:

$$\frac{dV}{dt} = \frac{1}{\beta_r} \frac{dP}{dt} + \frac{\Delta P}{\eta_r} - \alpha_r \frac{dT}{dt}, \quad (A4)$$

$$\frac{d\rho_m}{dt} = \frac{1}{\beta_m} \frac{dP}{dt} - \alpha_m \frac{dT}{dt}, \quad (A5)$$

$$\frac{d\rho_X}{dt} = \frac{1}{\beta_X} \frac{dP}{dt} - \alpha_X \frac{dT}{dt}, \quad (A6)$$

with α and β the thermal expansion coefficient (10^{-5} K^{-1}) and bulk modulus (10^{10} Pa) of the melt phase (m), crystal phase (X), and the mush/country rock (r). T indicates temperature, P stands for pressure, and ΔP denotes the overpressure, i.e., the pressure relative to the lithostatic pressure. η_r is the mush/country rock viscosity. From equations (A1) to (A6), one can derive a set of six coupled ordinary differential equations (ODE's) with six unknowns (pressure, temperature, gas volume fraction, volume, melt, and crystal density), which are solved using the ode15s subroutine in Matlab (Shampine & Reichelt, 1997), which is particularly well suited for stiff ordinary differential equations. Closure equations that describe volatile exsolution/dissolution (equation (B5)), crystallization/melting, and the gas density (equation (B6)) as described in the main text accompany this set of ODE's. We follow the description of the original model (Degruyter & Huber, 2014) for these.

Appendix B: Minimum Gas Volume Fraction Prior to Recharge

Leading up to an eruption, the magma chamber pressurizes from 155 to 195 MPa (lithostatic + critical overpressure) thereby reducing the gas volume fraction. In order for a magma to maintain a gas phase during a recharge event leading up to an eruption, there must be sufficient volatiles exsolved prior to the recharge.

We estimate the minimum amount of gas ϵ_{g0} necessary for this to occur using the mass balance of water. We assume the amount of volatiles is dominated by water and the amount of water at the time of eruption M_1^w can be expressed as

$$M_1^w = M_0^w + M_{in}^w, \tag{B1}$$

with M_0^w the mass of water prior to the recharge event and M_{in}^w the mass of water added by the recharge prior to eruption. We can expand this expression as follows

$$\rho_{g1}\epsilon_{g1}V_1 + m_{eq1}\rho_{m1}(1-\epsilon_{g1}-\epsilon_{x1})V_1 = \rho_{g0}\epsilon_{g0}V_0 + m_{eq0}\rho_{m0}(1-\epsilon_{g0}-\epsilon_{x0})V_0 + M_{in}^w, \tag{B2}$$

with the first term on the left and right-hand side denoting the mass of the gas phase and the second term on the left and right-hand side being the mass of the dissolved water. m_{eq} is the mass fraction of water dissolved in the melt phase. The other symbols are defined earlier in the text with subscripts 0 and 1 indicating the values just prior to recharge and at eruption, respectively. The minimum amount of gas present ϵ_{g0} to maintain a gas phase during recharge can be obtained by setting $\epsilon_{g1}=0$, i.e., the gas phase disappears at the moment of eruption and thus

$$m_{eq1}\rho_{m1}(1-\epsilon_{g1}-\epsilon_{x1})V_1 = \rho_{g0}\epsilon_{g0}V_0 + m_{eq0}\rho_{m0}(1-\epsilon_{g0}-\epsilon_{x0})V_0 + M_{in}^w. \tag{B3}$$

We make some further simplifying assumptions: the melt phase is nearly incompressible $\rho_{m1}=\rho_{m0}=2,400 \text{ kg/m}^3$, the crystal volume fraction remains nearly constant $\epsilon_{x1}=\epsilon_{x0}=0.25$, and the recharge volume is small relative to the total volume of the chamber $V_1=V_0$, and $M_{in}^w=0$. We can then rewrite the above equation to find

$$\epsilon_{g0} = \frac{(m_{eq1}-m_{eq0})\rho_{m0}(1-\epsilon_{x0})}{\rho_{g0}-m_{eq0}\rho_{m0}} \tag{B4}$$

The dissolved water mass fractions can be estimated using the parameterized solubility curve (Dufek & Bergantz, 2005; Zhang, 1999)

$$m_{eq} = 10^{-2} \left(\begin{array}{l} p^{0.5} \left(0.4874 - \frac{608}{T} + \frac{489530}{T^2} \right) \\ + p \left(-0.06062 + \frac{135.6}{T} - \frac{69200}{T^2} \right) \\ + p^{1.5} \left(0.00253 - \frac{4.154}{T} + \frac{1509}{T^2} \right) \end{array} \right), \tag{B5}$$

for P and T in Pa and K, respectively. Although, there is some dependence on temperature, the solubility of water in a silicic melt is most strongly controlled by the pressure. We obtain $m_{eq0}=0.05$ and $(m_{eq1}-m_{eq0}) \approx 0.007$ for $P_1=195 \text{ MPa}$, $P_0=155 \text{ MPa}$ and a temperature range between 1100 and 1200 K. The initial gas density can be estimated from the parameterized equation of state for the gas phase (Halbach & Chatterjee, 1982; Huber et al., 2010)

$$\rho_g = 10^3 \left(-112.528T^{-0.381} + 127.811P^{-1.135} + 112.04T^{-0.411}P^{0.033} \right), \tag{B6}$$

with the units of ρ_g , P , and T in kg/m^3 , bar, and $^\circ\text{C}$, respectively. For the initial conditions $P_0=155 \text{ MPa}$ and $T_0=870^\circ\text{C}$, we have $\rho_{g0}=334 \text{ kg/m}^3$. Putting it all together in equation (B4), we obtain that ϵ_{g0} is about 0.06. Running these calculations using the model we get a value of about 0.07. The difference results from the simplifying assumptions used in the estimate compared to the model.

References

- Allan, A. S. R., Wilson, C. J. N., Millet, M. A., & Wysoczanski, R. J. (2012). The invisible hand: Tectonic triggering and modulation of a rhyolitic supereruption. *Geology*, 40(6), 563–566.
- Annen, C. (2009). From plutons to magma chambers: Thermal constraints on the accumulation of eruptible silicic magma in the upper crust. *Earth and Planetary Science Letters*, 284(3–4), 409–416.
- Bachmann, O., & Dungan, M. A. (2002). Temperature-induced Al-zoning in hornblendes of the Fish Canyon magma, Colorado. *American Mineralogist*, 87(8–9), 1062–1076.
- Blake, S. (1981). Volcanism and the dynamics of open magma chambers. *Nature*, 289(5800), 783–785.

Acknowledgments

Funding for this project was provided by NSF grant EAR-1426887 for Degruyter and Huber, SNF grant # 200020_165501 to Bachmann, NSF grant EAR-1426858 to Cooper and NSF grant EAR-1425491 to Kent. We thank Mike Cassidy, Marco Viccaro, and an anonymous reviewer for their constructive reviews. Data of model runs and Matlab scripts to produce Figures 2–6 are available at <https://sites.google.com/site/degruyterwim/> Degruyter_etal_GCubed_Quizapu_Data.zip

- Blake, S. (1984). Volatile oversaturation during the evolution of silicic magma chambers as an eruption trigger. *Journal of Geophysical Research*, 89(B10), 8237–8244.
- Bower, S. M., & Woods, A. W. (1997). Control of magma volatile content and chamber depth on the mass erupted during explosive volcanic eruptions. *Journal of Geophysical Research*, 102(B5), 10273–10290.
- Caricchi, L., Annen, C., Blundy, J., Simpson, G., & Pintel, V. (2014). Frequency and magnitude of volcanic eruptions controlled by magma injection and buoyancy. *Nature Geoscience*, 7, 126–130.
- Caricchi, L., & Blundy, J. (2015). Experimental petrology of monotonous intermediate magmas. *Geological Society Special Publications*, 422(1), 105–130.
- Cassidy, M., Castro, J. M., Helo, C., Troll, V. R., Deegan, F. M., Muir, D., . . . Mueller, S. P. (2016). Volatile dilution during magma injections and implications for volcano explosivity. *Geology*, 44(12), 1027–1030.
- Castro, J. M., Cordonnier, B., Tuffen, H., Tobin, M. J., Puskas, L., Martin, M. C., & Bechtel, H. A. (2012). The role of melt-fracture degassing in defusing explosive rhyolite eruptions at Volcán Chaitén. *Earth and Planetary Science Letters*, 333, 63–69.
- Cooper, K. M., & Kent, A. J. R. (2014). Rapid remobilization of magmatic crystals kept in cold storage. *Nature*, 506(7489), 480–483.
- Degruyter, W., Bachmann, O., Burgisser, A., & Manga, M. (2012). The effects of outgassing on the transition between effusive and explosive silicic eruptions. *Earth and Planetary Science Letters*, 349–350, 161–170.
- Degruyter, W., & Huber, C. (2014). A model for eruption frequency of upper crustal silicic magma chambers. *Earth and Planetary Science Letters*, 403, 117–130.
- Degruyter, W., Huber, C., Bachmann, O., Cooper, K. M., & Kent, A. J. R. (2016). Magma reservoir response to transient recharge events: The case of Santorini volcano (Greece). *Geology*, 44(1), 23–26.
- Dragoni, M., & Magnanensi, C. (1989). Displacement and stress produced by a pressurized, spherical magma chamber, surrounded by a viscoelastic shell. *Physics of the Earth and Planetary Interiors*, 56(3–4), 316–328.
- Druitt, T. H., Costa, F., Delouie, E., Dungan, M., & Scailliet, B. (2012). Decadal to monthly timescales of magma transfer and reservoir growth at a caldera volcano. *Nature*, 482(7383), 77–80.
- Dufek, J., & Bergantz, G. W. (2005). Transient two-dimensional dynamics in the upper conduit of a rhyolitic eruption: A comparison of closure models for the granular stress. *Journal of Volcanology and Geothermal Research*, 143, 113–132.
- Edmonds, M., Humphreys, M. C. S., Hauri, E. H., Herd, R. A., Wadge, G., Rawson, H., . . . Guida, R. (2014). Chapter 16 Pre-eruptive vapour and its role in controlling eruption style and longevity at Soufriere Hills Volcano. *Geological Society Memoirs*, 39(1), 291–315.
- Eichelberger, J. C., Carrigan, C. R., Westrich, H. R., & Price, R. H. (1986). Non-explosive silicic volcanism. *Nature*, 323, 598–602.
- Gelman, S. E., Gutierrez, F. J., & Bachmann, O. (2013). On the longevity of large upper crustal silicic magma reservoirs. *Geology*, 41(7), 759–762.
- Girard, G., & Stix, J. (2009). Magma recharge and crystal mush rejuvenation associated with early post-collapse upper basin member Rhyolites, Yellowstone Caldera, Wyoming. *Journal of Petrology*, 50(11), 2095–2125.
- Gonnermann, H. M., & Manga, M. (2003). Explosive volcanism may not be an inevitable consequence of magma fragmentation. *Nature*, 426(6965), 432–435.
- Gregg, P. M., de Silva, S. L., Grosfils, E. B., & Parmigiani, J. P. (2012). Catastrophic caldera-forming eruptions: Thermomechanics and implications for eruption triggering and maximum caldera dimensions on Earth. *Journal of Volcanology and Geothermal Research*, 241–242, 1–12.
- Grosfils, E. B. (2007). Magma reservoir failure on the terrestrial planets: Assessing the importance of gravitational loading in simple elastic models. *Journal of Volcanology and Geothermal Research*, 166(2), 47–75.
- Grosfils, E. B., McGovern, P. J., Gregg, P. M., Galgana, G. A., Hurwitz, D. M., Long, S. M., & Chestler, S. R. (2015). Elastic models of magma reservoir mechanics: A key tool for investigating planetary volcanism. *Geological Society Special Publications*, 401(1), 239–267.
- Gudmundsson, A. (2012). Magma chambers: Formation, local stresses, excess pressures, and compartments. *Journal of Volcanology and Geothermal Research*, 237–238, 19–41.
- Halbach, H., & Chatterjee, N. D. (1982). An empirical Redlich-Kwong Equation of State for Water to 1000°C and 200 kbar. *Contributions to Mineralogy and Petrology*, 79, 337–345.
- Hildreth, W., & Drake, R. E. (1992). Volcán Quizapu, Chilean Andes. *Bulletin of Volcanology*, 54, 93–125.
- Huber, C., Bachmann, O., & Manga, M. (2009). Homogenization processes in silicic magma chambers by stirring and mushification (latent heat buffering). *Earth and Planetary Science Letters*, 283(1–4), 38–47.
- Huber, C., Bachmann, O., & Manga, M. (2010). Two competing effects of volatiles on heat transfer in crystal-rich magmas: Thermal insulation vs defrosting. *Journal of Petrology*, 51(4), 847–867.
- Huppert, H. E., & Woods, A. W. (2002). The role of volatiles in magma chamber dynamics. *Nature*, 420(6915), 493–495.
- Jaupart, C., & Allegre, C. J. (1991). Gas content, eruption rate and instabilities of eruption regime in silicic volcanoes. *Earth and Planetary Science Letters*, 102(3–4), 413–429.
- Jellinek, A. M., & DePaolo, D. J. (2003). A model for the origin of large silicic magma chambers: precursors of caldera-forming eruptions. *Bulletin of Volcanology*, 65, 363–381.
- Johnson, D. J. (1992). Dynamics of magma storage in the summit reservoir of Kilauea Volcano, Hawaii. *Journal of Geophysics Res*, 97(B2), 1807–1820.
- Karakas, O., Degruyter, W., Bachmann, O., & Dufek, J. (2017). Lifetime and size of shallow magma bodies controlled by crustal-scale magmatism. *Nature Geoscience*, 10(6), 446–450.
- Karlstrom, L., Dufek, J., & Manga, M. (2010). Magma chamber stability in arc and continental crust. *Journal of Volcanology Geothermal Research*, 190(3–4), 249–270.
- Kilbride, B. M., Edmonds, M., & Biggs, J. (2016). Observing eruptions of gas-rich compressible magmas from space. *Nature Communications*, 7, 13744.
- Klemetti, E. W., & Clynne, M. A. (2014). Localized rejuvenation of a crystal mush recorded in zircon temporal and compositional variation at the Lassen volcanic center, Northern California. *PLoS One*, 9(12), e113157.
- Koleszar, A. M., Kent, A. J. R., Wallace, P. J., & Scott, W. E. (2012). Controls on long-term low explosivity at andesitic arc volcanoes: Insights from Mount Hood, Oregon. *Journal of Volcanology Geothermal Research*, 219–220, 1–14.
- Kozono, T., & Koyaguchi, T. (2009). Effects of relative motion between gas and liquid on 1-dimensional steady flow in silicic volcanic conduits: 2. Origin of diversity of eruption styles. *Journal of Volcanology Geothermal Research*, 180(1), 37–49.
- Lejeune, A.-M., & Richet, P. (1995). Rheology of crystal-bearing silicate melts; an experimental study at high viscosities. *Journal of Geophysical Research*, 100(3), 4215–4229.
- Mader, H. M., Llewellyn, E. W., & Mueller, S. P. (2013). The rheology of two-phase magmas: A review and analysis. *Journal of Volcanology Geothermal Research*, 257, 135–158.

- Malfait, W. J., Seifert, R., Petitgirard, S., Perrillat, J.-P., Mezouar, M., Ota, T., . . . Sanchez-Valle, C. (2014). Supervolcano eruptions driven by melt buoyancy in large silicic magma chambers. *Nature Geoscience*, 7, 122–125.
- Manga, M., & Brodsky, E. (2006). Seismic triggering of eruptions in the far field: Volcanoes and geysers. *Annual Review of Earth and Planetary Sciences*, 34, 263–291.
- Marsh, B. D. (1981). On the crystallinity, probability of occurrence, and rheology of lava and magma. *Contributions to Mineralogy and Petrology*, 78, 85–98.
- Martin, V. M., Morgan, D. J., Jerram, D. A., Caddick, M. J., Prior, D. J., & Davidson, J. P. (2008). Bang! Month-scale eruption triggering at Santorini Volcano. *Science*, 321(5893), 1178.
- Menand, T., Annen, C., & de Saint Blanquat, M. (2015). Rates of magma transfer in the crust: Insights into magma reservoir recharge and pluton growth. *Geology*, 43(3), 199–202.
- Molloy, C., Shane, P., & Nairn, I. (2008). Pre-eruption thermal rejuvenation and stirring of a partly crystalline rhyolite pluton revealed by the Earthquake Flat Pyroclastics deposits, New Zealand. *Journal of the Geological Society*, 165, 435–447.
- Morgan, D. J., Blake, S., Rogers, N. W., De Vivo, B., Rolandi, G., & Davidson, J. P. (2006). Magma chamber recharge at Vesuvius in the century prior to the eruption of A.D. 79. *Geology*, 34(10), 845–848.
- Murphy, M. D., Sparks, R. S. J., Barclay, J., Carroll, M. R., & Brewer, T. S. (2000). Remobilization of andesitic magma by intrusion of mafic magma at the Soufrière Hills Volcano, Montserrat, West Indies. *Journal of Petrology*, 41(1), 21–42.
- Pallister, J. S., Hoblitt, R. P., & Reyes, A. G. (1992). A basalt trigger for the 1991 eruptions of Pinatubo volcano? *Nature*, 356, 426–428.
- Parks, M. M., Biggs, J., England, P., Mather, T. A., Nomikou, P., Palamartchouk, K., . . . Zacharis, V. (2012). Evolution of Santorini Volcano dominated by episodic and rapid fluxes of melt from depth. *Nature Geoscience*, 5(10), 749–754.
- Parmigiani, A., Degruyter, W., Leclaire, S., Huber, C., & Bachmann, O. (2017). The mechanics of shallow magma reservoir outgassing. *Geochemistry, Geophysics, Geosystems*, 18, 2887–2905. <https://doi.org/10.1002/2017GC006912>
- Parmigiani, A., Faroughi, S., Huber, C., Bachmann, O., & Su, Y. (2016). Bubble accumulation and its role in the evolution of magma reservoirs in the upper crust. *Nature*, 532(7600), 492–495.
- Pistone, M., Caricchi, L., Ulmer, P., Burlini, L., Ardia, P., Reusser, E., . . . & Arbaret, L. (2012). Deformation experiments of bubble- and crystal-bearing magmas: Rheological and microstructural analysis. *Journal of Geophysical Research*, 117, B05208. <https://doi.org/10.1029/2011JB008986>
- Rivalta, E., & Segall, P. (2008). Magma compressibility and the missing source for some dike intrusions. *Geophysical Research Letters*, 35, L04306. <https://doi.org/10.1029/2007GL032521>
- Roggensack, K., Hervig, R. L., McKnight, S. B., & Williams, S. N. (1997). Explosive basaltic volcanism from Cerro Negro volcano: Influence of volatiles on eruptive style. *Science*, 277, 1639–1642.
- Rubin, A. M. (1995). Propagation of magma-filled cracks. *Annual Review of Earth and Planetary Sciences*, 23, 287–336.
- Ruprecht, P., & Bachmann, O. (2010). Pre-eruptive reheating during magma mixing at Quizapu volcano and the implications for the explosiveness of silicic arc volcanoes. *Geology*, 38(10), 919–922.
- Ruprecht, P., Bergantz, G. W., Cooper, K. M., & Hildreth, W. (2012). The crustal magma storage system of Volcán Quizapu, Chile, and the effects of magma mixing on magma diversity. *Journal of Petrology*, 53(4), 801–840.
- Ruprecht, P., & Cooper, K. M. (2012). Integrating the uranium-series and elemental diffusion geochronometers in mixed magmas from Volcán Quizapu, Central Chile. *Journal of Petrology*, 53(4), 841–871.
- Shampine, L. F., & Reichelt, M. W. (1997). The MATLAB ODE suite. *SIAM Journal on Scientific Computing*, 18(1), 1–22.
- Sparks, R. S. J., Sigurdsson, H., & Wilson, L. (1977). Magma mixing: A mechanism for triggering explosive eruptions. *Nature*, 267, 315–318.
- Stock, M. J., Humphreys, M. C. S., Smith, V. C., Isaia, R., & Pyle, D. M. (2016). Late-stage volatile saturation as a potential trigger for explosive volcanic eruptions. *Nature Geoscience*, 9(3), 249–U290.
- Taisne, B., Tait, S., & Jaupart, C. (2011). Conditions for the arrest of a vertical propagating dyke. *Bulletin of Volcanology*, 73(2), 191–204.
- Tait, S., Jaupart, C., & Vergnolle, S. (1989). Pressure, gas content and eruption periodicity of a shallow, crystallising magma chamber. *Earth and Planetary Science Letters*, 92(1), 107–123.
- Till, C. B., Vazquez, J. A., & Boyce, J. W. (2015). Months between rejuvenation and volcanic eruption at Yellowstone caldera, Wyoming. *Geology*, 43(8), 695–698.
- Truby, J. M., Mueller, S. P., Llewellyn, E. W., & Mader, H. M. (2015). The rheology of three-phase suspensions at low bubble capillary number. *Proceedings of the Royal Society A Mathematical, Physical and Engineering Sciences/The Royal Society*, 471(2173), 20140557. <http://doi.org/10.1098/rspa.2014.0557>
- Villemant, B., & Boudon, G. (1998). Transition from dome-forming to Plinian eruptive styles controlled by H₂O and Cl degassing. *Nature*, 392(6671), 65–69.
- Vona, A., Di Piazza, A., Nicotra, E., Romano, C., Viccaro, M., & Giordano, G. (2017). The complex rheology of megacryst-rich magmas: The case of the mugearitic “cicirara” lavas of Mt. Etna volcano. *Chemical Geology*, 458, 48–67.
- Watts, R. B., de Silva, S. L., Jimenez de Rios, G., & Croudace, I. (1999). Effusive eruption of viscous silicic magma triggered and driven by recharge: a case study of the Cerro Chascon-Runtu Jarita Dome Complex in Southwest Bolivia. *Bulletin of Volcanology*, 61(4), 241–264.
- Wiebe, R. A., Manon, M. R., Hawkins, D. P., & McDonough, W. F. (2004). Late-stage mafic injection and thermal rejuvenation of the Vinalhaven Granite, Coastal Maine. *Journal of Petrology*, 45(11), 2133–2153.
- Woods, A. W., & Koyaguchi, T. (1994). Transitions between explosive and effusive eruptions of silicic magmas. *Nature*, 370, 641–644.
- Zhang, Y. X. (1999). Exsolution enthalpy of water from silicate liquids. *Journal of Volcanology and Geothermal Research*, 88(3), 201–207.